*International Journal of Thermophysics, Vol. 24, No. 6, November 2003 (© 2003)*

# Transient Behavior of a Thermoelectric Device under the Hyperbolic Heat Conduction Model

**M. Alata,[1] M. A. Al-Nimr,[1, 2] and M. Naji[1]**

*Received March 1, 2003*

The major objective of this work is to describe the dynamic thermal behavior of thermoelectric generators and refrigerators under the effect of the hyperbolic heat conduction model. In practical situations, these devices work under transient operating conditions due to the time change in the imposed current, voltage, and hot or cold temperatures. Results for transient temperature distributions were obtained for different parameters. The coefficient of performance was obtained as a function of time for increasing current flow.

**KEY WORDS:** dynamic behavior of heat pump; electrical generator and regenerator; hyperbolic heat conduction model; thermoelectric system.

## 1. INTRODUCTION

The basic theory of thermoelectric generators and refrigerators was derived satisfactorily in 1909 and 1911 by Altenkrich [1, 2]. His work indicated that for both applications materials were needed with high Seebeck coefficients to minimize Joule heating and low thermal conductivities to reduce heat transfer through the devices. Altenkirch [1, 2] enumerated the desirable properties for materials to be used in thermoelectric devices. In the literature, numerous studies have been conducted to investigate the thermal behavior of thermoelectric devices under steady-state conditions [3–11]. However, the behavior of these devices under transient operating conditions has not yet been investigated.

A study of the transient thermal behavior of the thermoelectric device rather than the steady-state behavior is very important for two reasons:

[1] Mechanical Engineering Department, Jordan University of Science and Technology (JUST), P.O. Box 3030, Irbid 22110, Jordan.

[2] To whom correspondence should be addressed. E-mail: malnimr@just.edu.jo



0195-928X/03/1100-1753/0 © 2003 Plenum Publishing Corporation

(a) to investigate the device behavior during the start-up and shut-down periods and (b) to understand the device thermal behavior when all or some of the operating conditions are varied with time. Examples of these operating conditions are the cold temperature, hot temperature, and the imposed electric field.

The thermoelectric transient behavior is investigated here using the hyperbolic heat conduction model. This model is more general than the parabolic (diffusion) heat conduction model. The parabolic diffusion model is considered as a special case of the hyperbolic model. The use of the hyperbolic model is essential in applications that involve imposed currents for very short durations and in applications that involve very thin *p*-type and *n*-type thermoelectric arrays. In addition, the hyperbolic model must be used when there are large temperature gradients within the device. Also, the hyperbolic model is important in order to understand the device behavior at very short times.

The major objective of this work is to describe the dynamic thermal behavior of thermoelectric generators and refrigerators. In practical situations, these devices work under transient operating conditions due to the transient behavior of the imposed current, voltage, and hot or cold temperatures.

## 2. ANALYSIS

Figure 1 is a schematic of a thermoelectric heat pump or refrigerator and involves a thermocouple composed of *n*- and *p*-type semiconductor elements placed electrically in series and thermally in parallel. When an electrical current $I$ flows through the circuit, the rates of heat rejection and input for operation between two reservoirs at $T_b$ and $T_c$ are $Q_h$ and $Q_c$, respectively. When the device is used as a heat pump, the reservoir at $T_h$ is the heated space and the rate of heat pumping is $Q_h$. When the device is used as a refrigerator, the reservoir at $T_c$ is the cooled space and the rate of refrigeration is $Q_c$. $T_1$ and $T_2$ are the temperatures inside the *n*- and *p*-type elements, respectively, and are functions of position $x$. $E$ is the emf of the external battery and provides the current $I$ to the circuit. Operation is based on the Peltier effect. At the same time, there are three additional effects [12, 13], namely, the Fourier, Joule, and Thomson effects.

It is assumed that the construction of the semiconductors is homogeneous; $k$ and $\sigma$ are constants. The lengths, uniform cross-sectional areas, thermal conductivities, electrical conductivities, Seebeck coefficients, and Thomson coefficients of *n*- (subscript 1) and *p*-type (subscript 2) elements are, respectively, $L_1$ and $L_2$, $A_1$ and $A_2$, $k_1$ and $k_2$, $\sigma_1$ and $\sigma_2$, $\alpha_1$ and $\alpha_2$, and

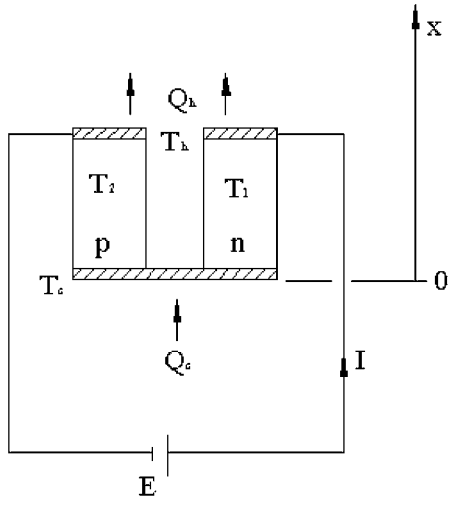


**Fig. 1.** Schematic of a thermoelectric heat pump or refrigerator.

$\gamma_1$ and $\gamma_2$. The elements are insulated, both electrically and thermally, from their surroundings except at the junction-reservoir contacts [14–17], and the temperature distribution inside the elements may be described by a one-dimensional heat-conduction model. Initially, both domains of the *n*- and *p*-type semiconductors are maintained at a uniform initial temperature $T_i$, and suddenly, a constant current $I$ flows into the circuit as shown in Fig. 1. The energy equation under the hyperbolic heat conduction model that describes the thermal behaviour of the system is given as [3]

$$\rho c \frac{\partial T}{\partial t} + \frac{\partial q}{\partial x} + eJ_N \frac{\partial \phi}{\partial x} = 0 \tag{1}$$

where

$$q(t+\bar{\tau}) = -k \frac{\partial T}{\partial x} + T\varepsilon e J_N \tag{2}$$

The Taylor expansion of Eq. (2) for $q(t+\bar{\tau})$ gives

$$q(t+\bar{\tau}) \approx q(t) + \bar{\tau} \frac{\partial q(t)}{\partial t}$$

Then Eq. (2) becomes:

$$q+\bar{\tau}\frac{\partial q}{\partial t}=-k\frac{\partial T}{\partial x}+T\varepsilon eJ_N \tag{3}$$

but

$$\frac{\partial \phi}{\partial x}=-\frac{eJ_N}{k_e}-\varepsilon\frac{\partial T}{\partial x} \tag{4}$$

where $k_e$ is the electrical conductivity. Now Eq. (3) is derived with respect to $x$:

$$\frac{\partial q}{\partial x}+\bar{\tau}\frac{\partial^2 q}{\partial t\,\partial x}=-\frac{\partial}{\partial x}\left(k\frac{\partial T}{\partial x}\right)+\frac{\partial}{\partial x}(T\varepsilon eJ_N) \tag{5}$$

From Eq. (1),

$$\frac{\partial q}{\partial x}=-\rho c\frac{\partial T}{\partial t}-eJ_N\frac{\partial \phi}{\partial x}$$

Substitution of $\frac{\partial q}{\partial x}$ in Eq. (5) yields

$$-\rho c\frac{\partial T}{\partial t}-eJ_N\frac{\partial \phi}{\partial x}-\bar{\tau}\rho c\frac{\partial^2 T}{\partial t^2}-\bar{\tau}e\frac{\partial}{\partial t}\left(J_N\frac{\partial \phi}{\partial x}\right)=-\frac{\partial}{\partial x}\left(k\frac{\partial T}{\partial x}\right)+\frac{\partial}{\partial x}(T\varepsilon eJ_N) \tag{6}$$

Substitution for $\frac{\partial \phi}{\partial x}$ from Eq. (4), with the notation that $\frac{\partial}{\partial x}(T\varepsilon eJ_N)=\varepsilon eJ_N\frac{\partial T}{\partial x}+(TeJ_N)\frac{\partial \varepsilon}{\partial x}$, where $J_N=J_N(t)$ only, gives

$$-\rho c\frac{\partial T}{\partial t}+\frac{e^2J_N^2}{k_e}-\bar{\tau}\rho c\frac{\partial^2 T}{\partial t^2}+\bar{\tau}\frac{\partial}{\partial t}\left[\frac{e^2J_N^2}{k_e}+\varepsilon eJ_N\frac{\partial T}{\partial x}\right]$$
$$=-\frac{\partial}{\partial x}\left(k\frac{\partial T}{\partial x}\right)+TeJ_N\frac{\partial \varepsilon}{\partial x} \tag{7}$$

but $I$ (current in amperes) $=eJ_NA$, where $A$ is the cross-sectional area. Also, $T\frac{\partial \varepsilon}{\partial x}=T\frac{\partial \varepsilon}{\partial T}\frac{\partial T}{\partial x}=\gamma\frac{\partial T}{\partial x}$, where $\gamma=T\frac{\partial \varepsilon}{\partial T}$ is the Thomson coefficient. Equation (7) becomes

$$\frac{\partial}{\partial x}\left(kA\frac{\partial T}{\partial x}\right)\mp\gamma I\frac{\partial T}{\partial x}+\frac{I^2}{RL}-\rho cA\frac{\partial T}{\partial t}-\bar{\tau}\rho cA\frac{\partial^2 T}{\partial t^2}+\bar{\tau}\frac{\partial}{\partial t}\left[\frac{I^2}{RL}\mp\varepsilon I\frac{\partial T}{\partial x}\right]=0 \tag{8}$$

where $R = \frac{4k_e}{L}$ is the electric resistance and $L$ is the domain length. The transient heat conduction equation inside the $n$- and $p$-type semiconductors is given by

$$\frac{\partial}{\partial x}\left(k_i A_i \frac{\partial T_i}{\partial x}\right) \mp \gamma_i I \frac{\partial T_i}{\partial x} + \frac{I^2}{R_i L_i} - \rho_i c_i A_i \frac{\partial T_i}{\partial t} - \bar{\tau}_i \rho_i c_i A_i \frac{\partial^2 T_i}{\partial t^2}$$

$$+ \bar{\tau}_i \frac{\partial}{\partial t}\left[\frac{I^2}{R_i L_i} \mp \varepsilon_i I \frac{\partial T_i}{\partial x}\right] = 0 \tag{9}$$

where $i = 1$ for the $n$-type semiconductor and $i = 2$ for the $p$-type. Also, the plus sign is for the $n$-type and the minus sign is for the $p$-type. Equation (9) assumes the following initial and boundary conditions:

$$\begin{gathered} T_1(0, x) = T_2(0, x) = T_i \\ \frac{\partial T_1}{\partial t}(0, x) = \frac{\partial T_2}{\partial t}(0, x) = 0 \\ T_1(t, 0) = T_2(t, 0) = T_c \\ T_1(t, L_1) = T_2(t, L_2) = T_h \end{gathered} \tag{10}$$

The transient behavior of the device is due to a suddenly imposed electric current. Initially, there is no electric current flowing within the device and the device temperature is equal to the ambient value. Suddenly, a constant electric current, in the form of a unit step function, is imposed on the system and one end is maintained at the cold temperature and the other is maintained at the hot temperature. As a result, the temperatures within the $n$-type and $p$-type domains, and the heating and cooling effects of the device, will be time dependent.

The thermoelectric device may be considered as a heat pump or refrigerator. When the device is used as a heat pump, the reservoir at $T_h$ is the heated space and the rate of heat pumping is $Q_h$. When the device is used as a refrigerator, the reservoir at $T_c$ is the cooled space and the rate of refrigeration is $Q_c$. The given governing equations apply for both cases, but the definition of the coefficient of performance differs between the two cases.

Equations (9) and (10) can be solved to determine the temperature distribution within each domain. In terms of the obtained temperature

distributions, one may define both heating and cooling effects of the thermoelectric device as

$$q_c = (\varepsilon_2^c - \varepsilon_1^c)\, T_c I - k_1 A_1 \frac{\partial T_1}{\partial x}(t, 0) - k_2 A_2 \frac{\partial T_2}{\partial x}(t, 0) \tag{11}$$

$$q_h = (\varepsilon_2^h - \varepsilon_1^h)\, T_h I - k_1 A_1 \frac{\partial T_1}{\partial x}(t, L_1) - k_2 A_2 \frac{\partial T_2}{\partial x}(t, L_2) \tag{12}$$

and the coefficient of performance (COP) is defined as

$$\Psi(t) = \frac{q_h}{q_h - q_c} \tag{13a}$$

For the case where the device is considered as a refrigerator, then the COP will be

$$\Psi(t) = \frac{q_c}{q_h - q_c} \tag{13b}$$

Now, using the dimensionless parameters defined in the Nomenclature, Eqs. (9) to (13a) are rewritten as

$$\frac{\partial^2 \theta_1}{\partial \xi^2} + F_1 \frac{\partial \theta_1}{\partial \xi} + F_2 - \frac{\partial \theta_1}{\partial \eta} - \tau_1 \frac{\partial^2 \theta_1}{\partial \eta^2} + \tau_1 \frac{\partial}{\partial \eta}\left[ F_2 - \frac{\varepsilon_1}{\gamma_1} F_1 \frac{\partial \theta_1}{\partial \xi} \right] = 0 \tag{14}$$

$$\alpha_R \frac{\partial^2 \theta_2}{\partial \xi^2} - E_1 \frac{\partial \theta_2}{\partial \xi} + E_2 - \frac{\partial \theta_2}{\partial \eta} - \tau_2 \frac{\partial^2 \theta_2}{\partial \eta^2} + \tau_2 \frac{\partial}{\partial \eta}\left[ E_2 + \frac{\varepsilon_2}{\gamma_2} E_1 \frac{\partial \theta_2}{\partial \xi} \right] = 0 \tag{15}$$

$$\begin{aligned} &\theta_1(0, \xi) = \theta_2(0, \xi) = 0 \\ &\frac{\partial \theta_1}{\partial \eta}(0, \xi) = \frac{\partial \theta_2}{\partial \eta}(0, \xi) = 0 \\ &\theta_1(\eta, 0) = \theta_2(\eta, 0) = 1 \\ &\theta_1(\eta, 1) = \theta_2(\eta, L_R) = r \end{aligned} \tag{16}$$

$$Q_c = M - \frac{\partial \theta_1}{\partial \xi}(\eta, 0) - k_R A_R \frac{\partial \theta_2}{\partial \xi}(\eta, 0) \tag{17}$$

$$Q_h = N - \frac{\partial \theta_1}{\partial \xi}(\eta, 1) - k_R A_R \frac{\partial \theta_2}{\partial \xi}(\eta, L_R) \tag{18}$$

and

$$\Psi = \frac{Q_h}{Q_h - Q_c} \tag{19}$$

where

$$\begin{aligned}
F_1 &= \frac{I\gamma_1 L_1}{A_1 k_1}, \qquad F_2 = \frac{I^2 L_1}{R_1(T_c - T_i)\, A_1 k_1}, \\
E_1 &= \frac{I\gamma_2 L_1}{C_R A_2 k_1}, \qquad E_2 = \frac{I^2 L_1^2}{C_R L_2 R_2 (T_c - T_i)\, A_2 k_1}, \\
\alpha_R &= \frac{\alpha_2}{\alpha_1}, \qquad C_R = \frac{\rho_2 c_2}{\rho_1 c_1}, \qquad k_R = \frac{k_2}{k_1}, \\
A_R &= \frac{A_2}{A_1}, \qquad L_R = \frac{L_2}{L_1}, \qquad r = \frac{T_h - T_i}{T_c - T_i} \\
M &= (\varepsilon_2^c - \varepsilon_1^c)\, \frac{T_c I L_1}{k_1 A_1 (T_c - T_i)} \\
N &= (\varepsilon_2^h - \varepsilon_1^h)\, \frac{T_h I L_1}{k_1 A_1 (T_h - T_i)}
\end{aligned} \tag{20}$$

The parameter $M$ represents the dimensionless form of the energy released (or absorbed) at the cold junction due to the Peltier effect. On the other hand, the parameter $N$ represents the dimensionless form of the energy released (or absorbed) at the hot junction due to the Peltier effect. The energy is released at the junction if the device operates as a heating pump, and the energy is absorbed at the junction if the device operates as a refrigerator. In general, $Q_c$ (or $Q_h$) contains energy released (or absorbed) from three sources: the first due to the Peltier effect, the second due to the conducted energy to the first domain, and the third due to the conducted energy to the second domain.

Now, using the Laplace transform technique, and with the notation that $L\{\theta(\eta, \xi)\} = W(s, \xi)$, Eqs. (14) to (16) are transformed to

$$W_1(s, \xi) = P_{11} e^{\lambda_{11}\xi} + P_{12} e^{\lambda_{12}\xi} + \frac{F_2}{s(\tau_1 s^2 + s)} \tag{21}$$

$$W_1(0) = 1, \qquad W_1(1) = r$$

$$W_2(s, \xi) = P_{21} e^{\lambda_{21}\xi} + P_{22} e^{\lambda_{22}\xi} + \frac{E_2}{s(\tau_2 s^2 + s)} \tag{22}$$

$$W_2(0) = 1, \qquad W_2(L_R) = r$$

where

$$\lambda_{11} = \tfrac{1}{2}\left[-A_1 + \sqrt{A_1^2 - 4B_1}\right], \qquad \lambda_{12} = \tfrac{1}{2}\left[-A_1 - \sqrt{A_1^2 - 4B_1}\right],$$

$$\lambda_{21} = \tfrac{1}{2}\left[-A_2 + \sqrt{A_2^2 - 4B_2}\right], \qquad \lambda_{22} = \tfrac{1}{2}\left[-A_2 - \sqrt{A_2^2 - 4B_2}\right]$$

$$P_{11} = \frac{r - e^{\lambda_{12}}\left(1 - \dfrac{F_2}{s^2}\right) - \dfrac{F_2}{s^2}}{e^{\lambda_{11}} - e^{\lambda_{12}}}, \qquad P_{12} = 1 - \frac{F_2}{s^2} - P_{11}$$

$$P_{21} = \frac{r - e^{\lambda_{22} L_R}\left(1 - \dfrac{E_2}{s^2}\right) - \dfrac{E_2}{s^2}}{e^{\lambda_{21} L_R} - e^{\lambda_{22} L_R}}, \qquad P_{22} = 1 - \frac{E_2}{s^2} - P_{21}$$

$$A_1 = \left(1 - \tau_1 \frac{\varepsilon_1}{\gamma_1} s\right) F_1, \qquad B_1 = -(\tau_1 s^2 + s)$$

$$A_2 = \left(\frac{\tau_2 \varepsilon_2}{\gamma^2} s - 1\right) \frac{E_1}{\alpha_R}, \qquad B_2 = -\frac{(\tau_2 s^2 + s)}{\alpha_R}$$

Equations (21) and (22) are inverted in terms of the Riemann-sum approximation [18] as

$$F(\eta, \zeta) = \frac{e^{\gamma t}}{\mu}\left[\frac{1}{2}\bar{F}(\tau, \zeta) + \mathrm{Re}\sum_{n=1}^{N} \bar{F}\left(\tau + \frac{in\pi}{\mu}, \zeta\right)(-1)^n\right] \tag{23}$$

where $\bar{F}(\tau, \zeta)$ is the Laplace transform of $F(\eta, \zeta)$.

For faster convergence of Eq. (23), it has been shown [18] that $\gamma$ may be obtained from

$$\tau\zeta = 4.7$$

Expressions for $\theta_1$ and $\theta_2$ are obtained directly from Eqs. (20) and (21), respectively.

## 3. RESULTS AND CONCLUSION

The figures show the transient behavior of the thermoelectric generator or refrigerator. Data were obtained for the following parameters:

$\gamma_1 = \varepsilon_1 = 10^{-4}$, $L_R = k_1 = R = a_R = 1$, $E_1 = 0.625$, $F_1 = 0.313$, $M = 0.8$

$\gamma_2 = \varepsilon_2 = 2 \times 10^{-4}$, $r = 1.1$, $E_2 = F_2 = 100$, $N = 1.0$

$\tau_1 = \tau_2 = 10^{-4}$

Figure 2 shows the transient temperatures distribution ($\theta_1$ and $\theta_2$) at different axial locations. Figure 2a is for $\tau = 10^{-4}$, and Fig. 2b is for $\tau = 10^{-3}$. For the parameters selected in the analysis, both figures show no variation between $\theta_1$ and $\theta_2$. Also, both figures show that the rate of temperature increase is very high near the boundaries where it reaches maximum values in shorter times and continues to decrease but at a slower rate. However, this rate decreases when moving towards the center ($\xi \to 0.5$). As time proceeds, steady-state temperatures are achieved. Steady-state time increases when going from the boundaries towards the center since heat takes longer times to reach the center. Although the time required reaching steady-state behavior is relatively small, the effect of the short duration in transient behavior is of significant impact in applications involving fluctuating electrical current and a time-dependent electrical source, plus applications in control systems where a sudden change in current flow occurs. Comparisons of these figures show that an increase in $\tau$ gives higher temperature values at corresponding times. However, peak-temperature times and the times to reach steady state increase as $\tau$ increases. This is shown clearly in Fig. 2c for $\xi = 0.3$.

In Fig. 2, various peaks in the temperature transient behavior are due to the hyperbolic oscillatory behavior of the heat conduction model used here. The hyperbolic heat conduction model assumes that heat travels within the domain in the form of thermal waves that have finite speed. These thermal waves interfere in a constructive or destructive manner, and as a result, thermal waves travel within the domain with wavefronts. These traveling thermal waves make the appearance of such peaks possible. These peaks appear at certain locations at a given time and at other locations at other times. Also, the appearance of high temperature gradients within *n*- and *p*-type domains is a result of using the hyperbolic heat conduction model.

In Fig. 3, the axial temperature variation is plotted at different times for $\tau = 10^{-4}$. It is worth mentioning here that $\theta_1$ and $\theta_2$ temperatures are symmetric about $\xi = 0.5$, but in reverse directions and again no difference is observed between them for the selected parameters.

Figures 4 and 5 show the effects of $F_1$ and $F_2$, respectively, on the transient temperature behavior at $\xi = 0.3$. As expected from Eqs. (14) and (15), these parameters only affect the $\theta_1$ temperature distribution while having no effect on the $\theta_2$ temperature distribution. Figure 4 shows that an increase in $F_1$ by increasing the Thomson coefficient, for example, produces lower $\theta_1$ temperature values. This result shows that there is an adverse influence of the Thomson effect on the rate of heat pumping. However, Fig. 5 shows that an increase in $F_2$ by increasing the electrical conductivity or decreasing the electrical resistance R produces higher $\theta_1$ temperature

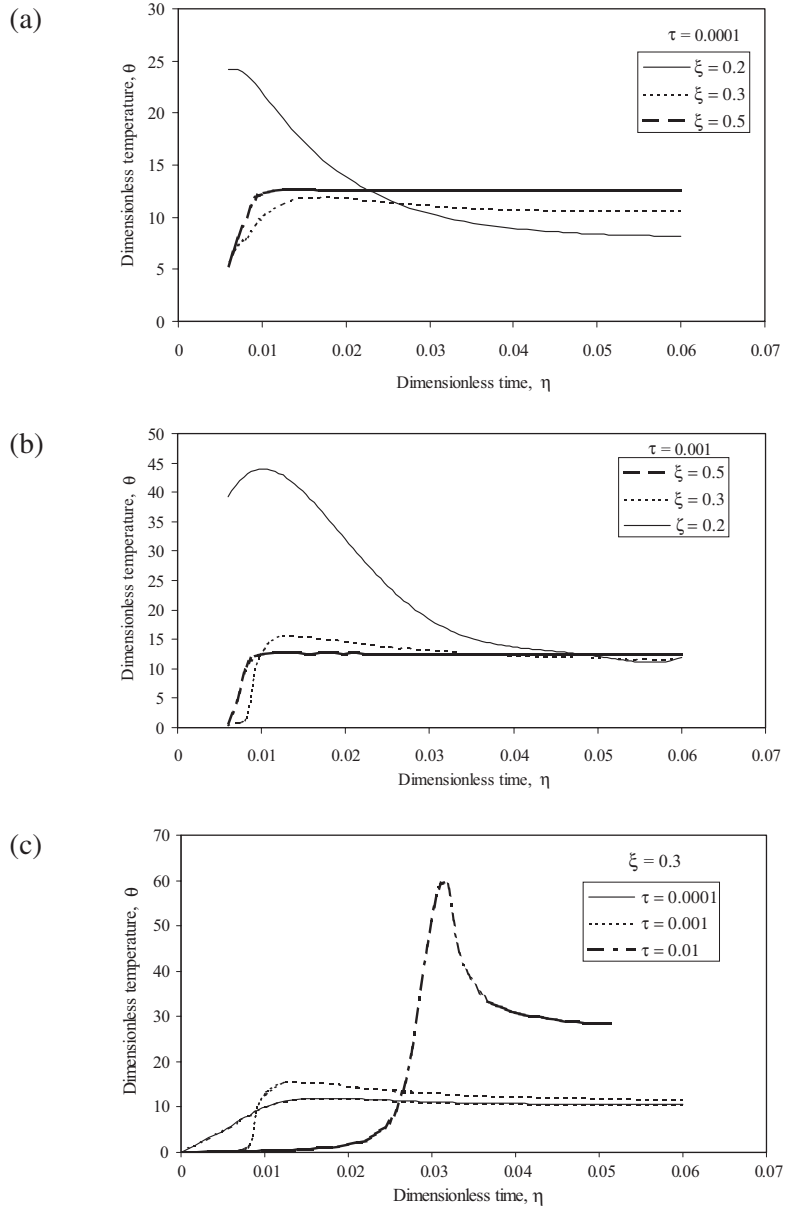


**Fig. 2.** (a) Transient temperature behavior at different locations for $\tau = 10^{-4}$; (b) transient temperature behavior at different locations for $\tau = 10^{-3}$; (c) transient temperature behavior for different t values at $\xi = 0.3$.

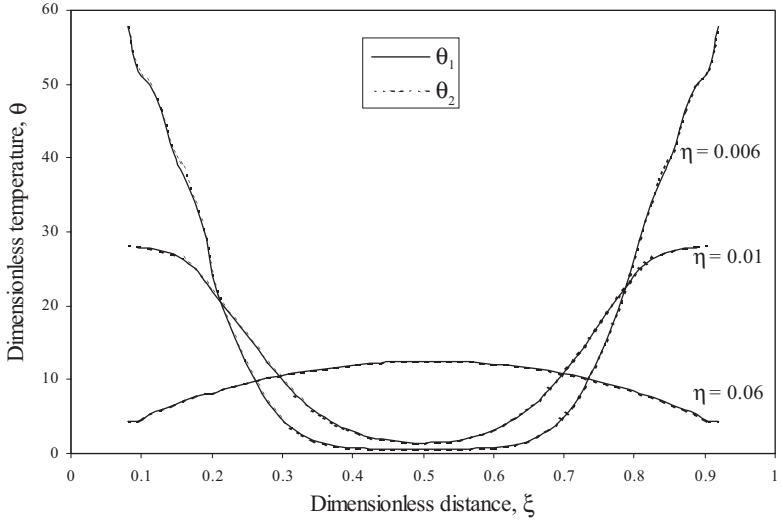


**Fig. 3.** Axial temperature distribution at different times.

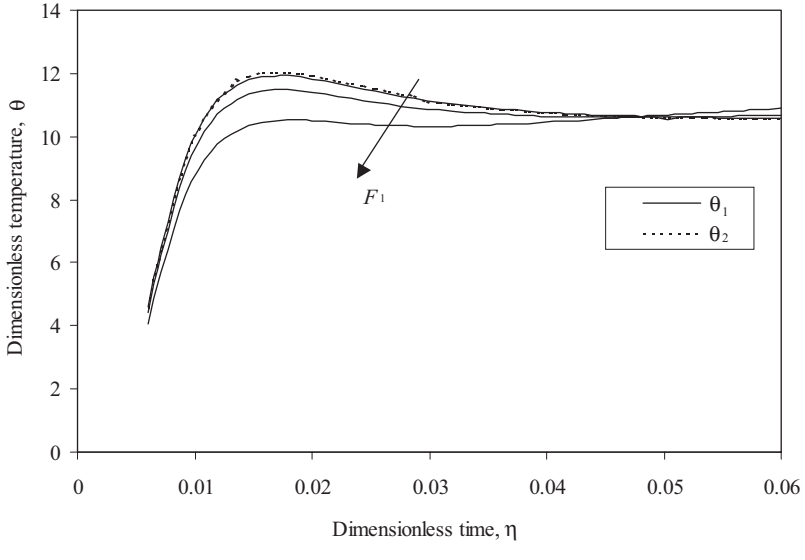


**Fig. 4.** Effect of $F_1$ on the transient temperature distribution at $\xi = 0.3$.

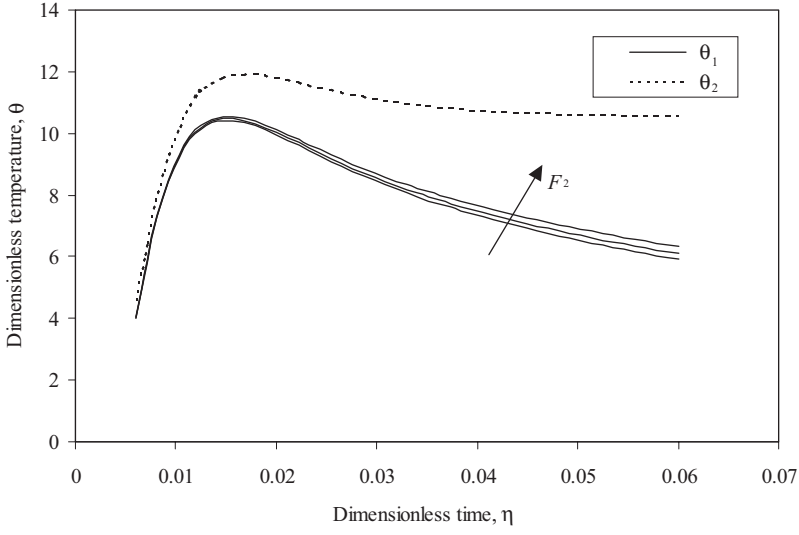


**Fig. 5.** Effect of $F_2$ on the transient temperature distribution at $\xi = 0.3$.

values. This is a direct consequence since an increase in electrical conductivity enhances thermal transport. Also, it can be seen that the *n*-type temperature $\theta_1$ values are lower than the *p*-type temperature $\theta_2$ values, as expected.

Similar results were obtained for the effect of $E_1$ and $E_2$ on the transient temperature behavior at $\xi = 0.3$ in Figs. 6 and 7, respectively. These parameters only affected the $\theta_2$ temperature distribution while having no effect on the $\theta_1$ temperature distribution, as can be seen from Eqs. (14) and (15). The same conclusions drawn for Figs. 4 and 5 apply for Figs. 6 and 7.

However, the behavior in Figs. 4 and 6 is different than that in Figs. 5 and 7. It is clear from Eqs. (14) and (15), and at large times, the governing equations become

$$\frac{\partial^2\theta_1}{\partial\xi^2} + F_1\frac{\partial\theta_1}{\partial\xi} + F_2 - \frac{\partial\theta_1}{\partial\eta} = 0, \qquad \alpha_R\frac{\partial^2\theta_2}{\partial\xi^2} - E_1\frac{\partial\theta_2}{\partial\xi} + E_2 - \frac{\partial\theta_2}{\partial\eta} = 0$$

Now, for most practical applications, $F_2$ and $E_2$ are much larger than $F_1$ and $E_1$ ($E_1 = 0.625$, $F_1 = 0.313$, $E_2 = F_2 = 100$), and as a result, the governing equations become

$$\frac{\partial^2\theta_1}{\partial\xi^2} + F_2 - \frac{\partial\theta_1}{\partial\eta} = 0, \qquad \alpha_R\frac{\partial^2\theta_2}{\partial\xi^2} + E_2 - \frac{\partial\theta_2}{\partial\eta} = 0$$

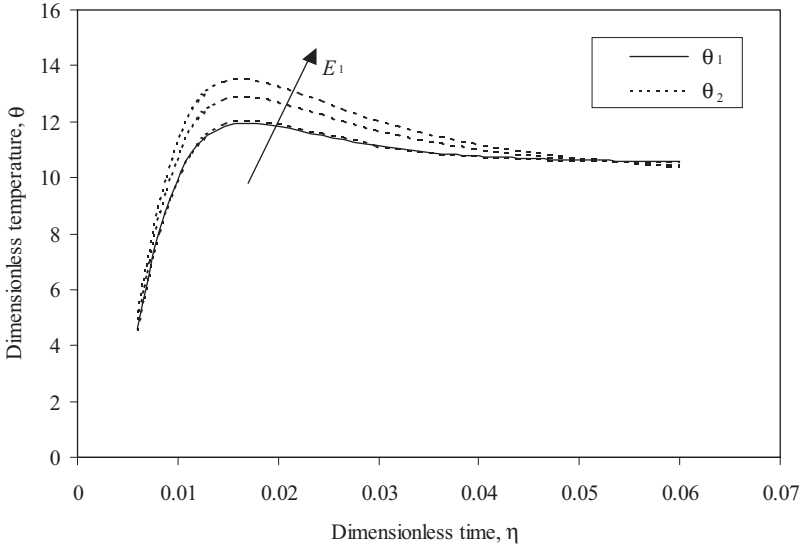


**Fig. 6.** Effect of $E_1$ on the transient temperature distribution at $\xi = 0.3$.

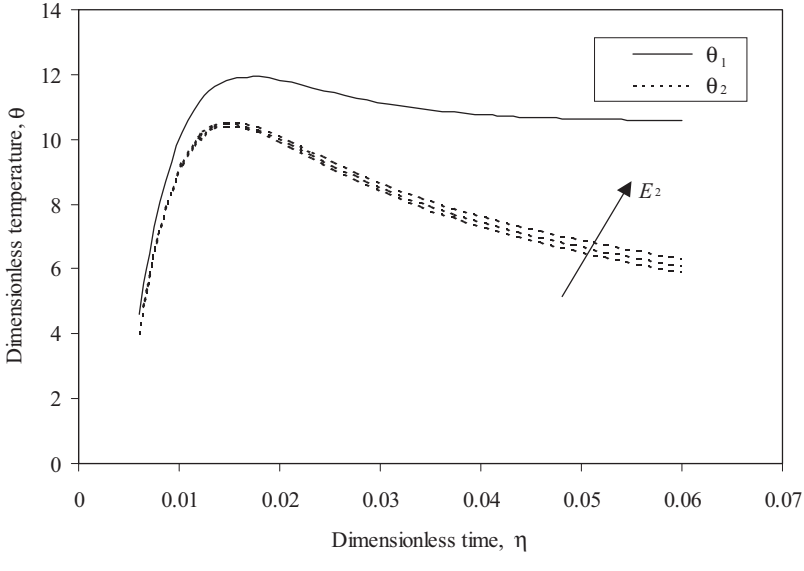


**Fig. 7.** Effect of $E_2$ on the transient temperature distribution at $\xi = 0.3$.

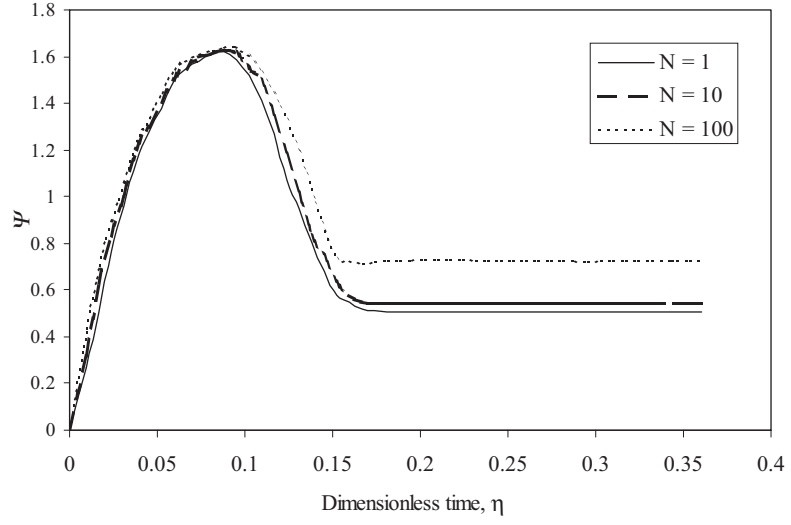


**Fig. 8.** Transient coefficient of performance variation at $\xi = 0.3$ for different $N$ values.

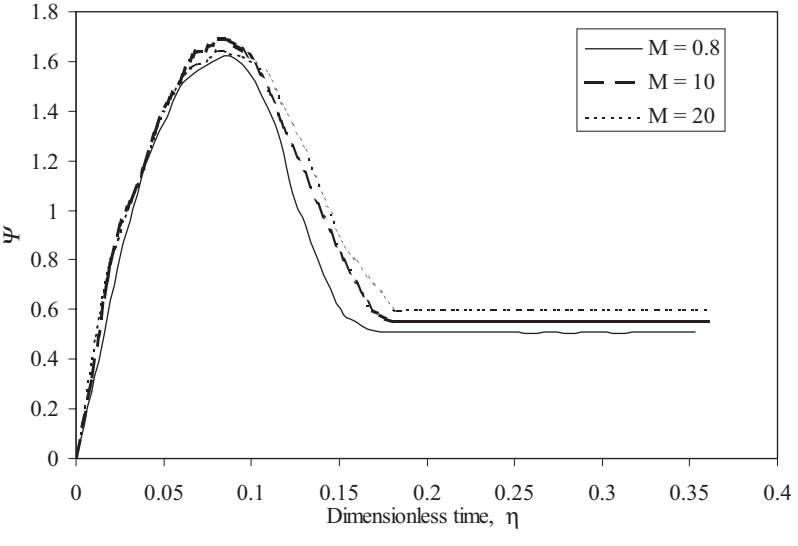


**Fig. 9.** Transient coefficient of performance variation at $\xi = 0.3$ for different $M$ values.

In Figs. 4 and 6 the results are estimated with the assumption that $F_2 = E_2 = 100$ and $a_R = 1$. As a result, both Eqs. (14) and (15) are the same at large values of time.

On the other hand, Figs. 5 and 7 are estimated at different values of $F_2$ and $E_2$, and this explains why the temperature of the first domain does not approach that of the second domain as time proceeds. However, and as clear from these two figures, the two temperatures approach each other as $F_2$ approaches $E_2$ or as $E_2$ approaches $F_2$.

In Figs. 8 and 9 the transient behavior of the coefficient of performance $\Psi$ is shown for different $N$ and $M$ values, respectively. The increase in $N$ or $M$ values can be due to the increase in current flow $I$ as can be seen from Eq. (20). In both figures, an increase in the current flow has negligible effect on $\Psi$ at short times where the increase in the rate of $\Psi$ is large. As time proceeds, $\Psi$ starts to decrease until it reaches a steady-state value. The steady-state $\Psi$ value increases with an increase in current flow $I$.

## NOMENCLATURE

| | |
|---|---|
| $A_R$ | Area ratio $A_2/A_1$ |
| $A$ | Cross-sectional area |
| $c$ | Specific heat capacity |
| $C$ | Total heat capacity, $\rho c$ |
| $C_R$ | Total heat capacity ratio, $C_2/C_1$ |
| $e$ | Electronic charge |
| $I$ | Electric current |
| $J_N$ | Current density |
| $k$ | Thermal conductivity |
| $k_e$ | Electrical conductivity |
| $k_R$ | Thermal conductivity ratio, $k_2/k_1$ |
| $L$ | Length |
| $L_R$ | Length ratio, $L_2/L_1$ |
| $q_c$ | Cooling effect of the device |
| $q_h$ | Heating effect of the device |
| $Q_c$ | Dimensionless cooling effect, $\dfrac{q_c L_1}{k_1 A_1 (T_c - T_\infty)}$ |
| $Q_h$ | Dimensionless heating effect, $\dfrac{q_c L_1}{k_1 A_1 (T_c - T_\infty)}$ |
| $r$ | Temperature ratio, $\dfrac{(T_h - T_\infty)}{(T_c - T_\infty)}$ |
| $R$ | Electric resistance, $\dfrac{Ak_e}{L}$ |
| $t$ | Time |

$T$ Temperature
$T_c$ Cold junction temperature
$T_h$ Hot junction temperature
$T_i$ Initial temperature
$x$ Spatial coordinate

## Greek Symbols

$\alpha$ Thermal diffusivity
$\alpha_R$ Thermal diffusivity ratio, $\alpha_1/\alpha_2$
$\varepsilon$ Seebeck coefficient
$\gamma$ Thomson Coefficient
$\eta$ Dimensionless time, $\dfrac{\alpha_1 t}{L_1^2}$
$\theta$ Dimensionless temperature, $\dfrac{(T-T_\infty)}{(T_c-T_\infty)}$
$\rho$ Density
$\bar{\tau}$ Thermal relaxation time
$\phi$ Electrostatic potential
$\xi$ Dimensionless spatial coordinate, $\dfrac{x}{L_1}$
$\psi$ Coefficient of performance, $\dfrac{q_h}{(q_h-q_c)}$

## REFERENCES


1. S. W. Angrist, *Direct Energy Conversion* (Allyn & Bacon, Boston, 1976).
2. A. Bejan, *Advanced Engineering Thermodynamics* (Wiley, New York, 1988).
3. J. Chen, Z. Yan, and L. Wu, *Energy* **22**:979 (1997).
4. B. Sherma, R. R. Heikes, and R. W. Ure, Jr., *J. Appl. Phys.* **31**:1 (1960).
5. A. H. Boerdijk, *J. Appl. Phys.* **30**:1080 (1959).
6. C. N. Rollinger, *J. Heat Transfer* **87**:259 (1965).
7. K. Landecker, in *Thermoelectric Energy Conversion,* K. R. Rao, ed. (IEEE, New York, 1976), pp. 150–154.
8. T. C. Harman, *J. Appl. Phys.* **29**:1471 (1958).
9. B. W. Swanson, E. V. Somers, and R. R. Heikes, *J. Heat Transfer* **83**:77 (1961).
10. H. J. Golsmid and R. W. Douglas, *Brit. J. Appl. Phys.* **5**:386 (1954).
11. N. A. Bayne, Jr., *Portable Thermoelectric Generators*, Paper No. 645A, Trans. SAE (1963).
12. M. J. Lampinen, *J. Appl. Phys.* **69**:4318 (1991).
13. M. Cvahte and J. Strnad, *Eur. J. Phys.* **9**:11 (1988).
14. J. M. Gordon, *Am. J. Phys.* **59**:551 (1991).
15. C. Wu, *Energy Conversion and Management* **34**:1239 (1993).
16. Z. Yan and J. Chen, *AIP Conf. Proc. (USA)* **316**:343 (1995).
17. J. Chen and B. Andersen, *Int. J. Ambient Energy* **17**:22 (1996).
18. D. Tzou, *Macro to Microscale Heat Transfer* (Taylor & Francis, Washington, D.C., 1997).